Research Article

# Investigation of Land Use and Land Cover Using Temporal Satellite Images Surrounding The Open Cast Coal Mining Project, Mancherial, Telangana (India)

Endapalli Mahendar, Mandela Govindaraj, Sandi Kumar Reddy*

National Institute of Technology Karnataka, Department of Mining Engineering, Surathkal, Karnataka, India-575025

Corresponding author: Sandi Kumar Reddy, Email: skreddy@nitk.edu.in

**Abstract:**

Land use and land cover (LULC) products play crucial for researching LULC change as well as environmental and social issues. Rapid changes in LULC brought on by industrial operations such as open-cast coal mining pose serious problems to natural ecosystems, requiring careful observation in order to manage the environment sustainably. Multi-temporal satellite imagery and spatial data analytical methods were used to assess Land Surface Temperature (LST) for the periods of 2021 to 2026. Supervised classification and evaluations in accuracy disclosed that the overall accuracies of Sentinel-2's sharper resolution and bands with red-edge was improved by 3–5%, especially for fine-scale characteristics, such as limits of mining areas. One of the most significant LULC transitions was a 23% change from agriculture and vegetation land to built-up regions, which reflected urbanization brought on by mining leads to temperature rise in Build-up/Barren land, decrease in vegetation cover around 75% and water bodies area increase around 24%. These results demonstrate the value of high-resolution images for environmental monitoring and the effectiveness of Remote Sensing and Geographic Information System approaches for LULC mapping in mining regions. This study supports data-driven mitigation of climate change and sustainable land management initiatives by providing a framework for decision-makers to solve environmental deprivation caused by mining.

**Keywords**: Land Surface Temperature (LST), Opencast Mining, Remote Sensing (RS), QGIS, Geographic Information System (GIS).

## 1. Introduction

Land use and land cover studies is essential in understanding developments in environment brought on by mankind activity and natural mechanism, including urbanization, changing the climate-induced temperature variations, and resource excavations. Precise mapping of LULC is essential for sustainable growth, as it will provide the information to implement the policies on forest conservation, vegetation management, agriculture activities, water resources data and its management, and natural resource preservation (Sridhar et al., 2019; Gond et al., 2026). LULC maps are vital for recognizing and provide the data of land cover classes such as water bodies, forest land/vegetation, agricultural land, built-up area, barren land, mining area, etc., and also gives agricultural suitability, watershed management, and assessing climate change impacts on temperature, air and water quality, groundwater, geomorphology, and socio-agricultural monitoring (Nugroho et al., 2023; Venter et al., 2022; Gorai et al., 2022; Chowdhuri et al., 2021; Mishra et al., 2020; Sujatha & Sridhar, 2018; Manna et al., 2014; Jinghua et al., 2011; Ghosh et al., 1990). Remote sensing (RS) has arisen as a main tool for observing LULC and LST shifts across large regions, providing an affordable and scalable means of capturing their temporal and spatial data changes (Liu et al., 2021). Despite its advantages, remote sensing is controlled by its limitations in spatial resolution constraints, temporal resolution issues, atmospheric interferences, cost and availability, data processing requirements, limited penetration capabilities, and legal and privacy concerns (Lokesh et al., 2023 & 2025; Ji et al., 2021; Kumar Reddy, 2016 & 2023; Wang et al., 2018; Workie & Debella, 2017; Mcconnell et al., 2002).

In coal mining areas such as the Mancherial region, Telangana, remote sensing with Sentinel-2 and Landsat data was used to analyse LULC classes and temperature dynamics during the opencast mining period, showing how mining activities and topography influence pollution and may alter LULC patterns. Open-cast coal mining is a main driver of LULC modification, causing deterioration of land quality, deforestation, land surface temperature, and urban expansion. The massive open-cast coal mining region in the Mancherial, Telangana, one of India's biggest coal generating areas, illustrating these consequences. Mining operations contribute to environmental degradation by changing vegetation and agriculture, especially through changes in LULC classes, land surface temperature fluctuations, and the dispersion of mining dust. Despite these results, there are still few thorough studies on the impact on environment of opencast coal mining in Mancherial area, particularly

those that incorporate long-term LULC trend study using multi-resolution satellite datasets. Most recent studies focus on contrasting machine learning (ML) classifications for land use land cover visualization, rarely addressing settings unique to mining or the combined impacts of mining vegetation land, dust, and air pollutants on changes in land cover. These gaps are reported in this study by employing remote sensing to interpret multispectral satellite data from Landsat-8 (15 m coverage) and Sentinel-2 (10 m coverage) for LULC classification across the Mancherial region, Telangana open-cast coal mining sector. The most accurate way to classify LULC into six classes—water bodies, forest land/vegetation, crop land/agriculture land, built-up area, barren land, and mining area—is determined by comparing the performance of classifiers. The study assess mining impacts by analyzing LULC transitions from 2021 to 2026 using a supervised classification approach, using QGIS maps for analysis of detection in change. This study offers new insights into the environmental impacts of open-cast coal mining and a paradigm for sustainable mining land management areas by incorporating multi-resolution imagery. Further-more, results aid in to comprehend the various scales at which LULC varies due to the extension of open-cast mining operations to deeper levels and associated land surface temperature variations in surrounding areas. The results of the study expose the important of spatial and temporal variations in LULC, and LST patterns in the study area. Remote sensing analysis using satellite datasets proved effective in capturing environmental changes associated with mining activities. The findings further suggest that topographic conditions and opencast coal mining operations play a major role in influencing pollution and subsequent LULC changing aspects. These findings show the potential of geospatial techniques for environmental monitoring and impact continuous assessment in open-cast coal mining regions.

## 2. Study Area

The project has a core area of 355.11 Hectares (Ha) and a total project area of 635.54 Hectares. It is situated in the southernmost part of the Somagudem–Indaram Coal Belt of Godavari Valley Coal Fields. The project area lies between North Latitude 18°46’30” to 18°52’00” and East Longitude 79°28’00” to 79°31’00”, falling in Survey of India Topo-sheet No. 56N/9 (Fig. 1).

The Mancherial Region of Telangana is a critical hub for coal-based energy production. To meet the growing demand for coal, large-scale mining through the Opencast Project, produces approximately 5,00,000 tonnes per year of coal, which is imperative to meet ongoing industrialisation demands. These operations, however, also introduce severe environmental and socioeconomic challenges.

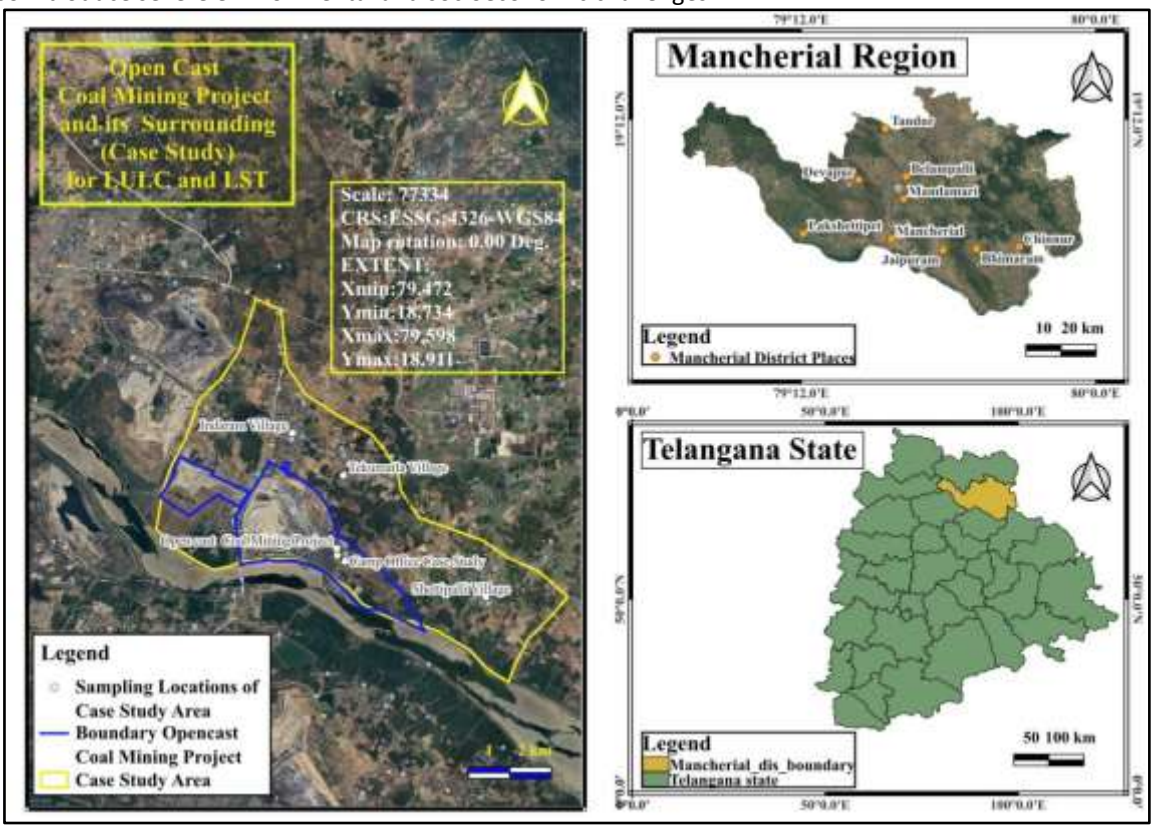



**Fig. 1. Open-cast mine location and area.**

The project boundaries are Indaram and Tekumatla villages on the north, Tekumatla Pedda Vagu on the east, the Godavari River on the south, and the State Highway on the west. The maximum depth of the proposed quarry is 250 m, and the mining life of the project is 26 years, including the construction period. The project falls in the Jaipur Mandal of the Mancherial region of Telangana. The production started from the year of 2020-21 with 10.01 lakh tonnes of coal production and 10.120 $m^3$ overburden is removed and continues further. The mining area expanded from 2021 to 2024. The mining area expanded around 26071200 $m^2$ during 2021 to 2026.

**Datasets**

Temporal satellite images from ESRI Sentinel-2 10m Resolution LULC were used to generate LULC maps through unsupervised maximum likelihood classification (https://livingatlas. arcgis.com/landcover/). LULC maps for 2021 to 2025 were validated through field observations, yielding an accuracy of 92%. These temporal datasets enabled the ongoing evaluation of land use dynamics and alterations in the area used for open-cast coal mining.

**Table I. Satellite datasets used for Open-cast mine area LULC and LST analysis.**

| Year | Data Source | Application |
|---|---|---|
| 2021 | Sentinel-2 (10m) | LULC classification |
| 2022 | Sentinel-2 (10m) | LULC classification |
| 2023 | Sentinel-2 (10m) | LULC classification |
| 2024 | Sentinel-2 (10m) | LULC classification |
| 2025 | Sentinel-2 (10m) | LULC classification |
| 2021 | Landsat 8-OLI (15m) | LST derivation |
| 2022 | Landsat 8-OLI (15m) | LST derivation |
| 2023 | Landsat 8-OLI (15m) | LST derivation |
| 2024 | Landsat 8-OLI (15m) | LST derivation |
| 2025 | Landsat 8-OLI (15m) | LST derivation |
| 2026 | Landsat 8-OLI (15m) | LST derivation |

Land Surface Temperature data were obtained from USGS earth explorer using Landsat 8-OLI for the years 2021 to 2026 at open-cast mine area (Table I). The radiative temperature, or LST, is determined by single-channel algorithms employing the top-of-atmosphere brightness temperature, emitted radiation wavelength, and land surface emissivity.

**4 Methodology**

***a)*** **Land Use Land Cover (LULC):**

Temporal satellite images from ESRI Sentinel-2, 10m resolution LULC was used to generate LULC maps through unsupervised maximum likelihood classification. The classified maps were validated through field observations. LULC classes identified include: water bodies, trees/forest land, bare land, barren land, and mining area.

***b)*** **Land Surface Temperature (LST):**

Landsat Band 6 (thermal infrared) is used for LST estimation.

Step 1: Digital Number (DN) to Radiance: Radiance is calculated using metadata calibration constants.

Step 2: Radiance to Brightness Temperature (BT):Brightness temperature is derived using thermal constants (K1 and K2): K1=607.76; K2=1260.56

Step 3: NDVI Calculation

Normalized Difference Vegetation Index is calculated as:

$$NDVI = \frac{NIR - RED}{NIR + RED}$$

NDVI is used to estimate vegetation density and emissivity

Step 4: Proportion of Vegetation (Pv)

$$P_v = \left( \frac{NDVI - NDVI_{min}}{NDVI_{max} - NDVI_{min}} \right)^2$$

Step 5: Land Surface Emissivity (LSE)

$$LSE = 0.004 \times Pv + 0.986$$

Step 6: Final LST Calculation

The final Land Surface Temperature is computed as:

$$\text{LST} = \frac{BT}{1+\left(\frac{\lambda \times BT}{\rho}\right)\ln(LSE)} - 273.15$$

where BT = Top-of-atmosphere Brightness Temperature (°C); λ = Wavelength of emitted radiance (Landsat 8 OLI & TIRS: 11.45µm); LSE = Land Surface Emissivity.

**Brightness Temperature (BT):**

Top-of-atmosphere BT was converted from spectral radiance to Celsius as:

$$BT = \frac{K_2}{\ln\left(\frac{K_1}{L_\lambda}+1\right)} - 273.15$$

where the thermal constants '$K_1$' and '$K_2$' from the metadata file and '$L_\lambda$' is TOA spectral radiance ($Wm^{-2}\,sr^{-1}\,\mu m^{-1}$).

LULC and LST maps are overlaid to analyze spatial relationships. Mean LST is calculated for each LULC class using zonal statistics:

- Built-up areas → highest temperature
- Trees / Forest Land / Vegetation → moderate temperature
- Water / Water bodies → lowest temperature

**Urban Heat Island (UHI) Analysis**: Hotspot regions are identified based on high LST values, particularly in urban/built-up zones.

For validation, land surface temperatures were measured in the field within a distance of 5 km covering the site office, camp office, mining area, nearby villages (Indaram Village, Nizambad palle Village, Shettipalli Village, and Tekumatla Village) using a portable LCD monitor thermometer. The general methodology for LST derivation is shown in Fig. 2.

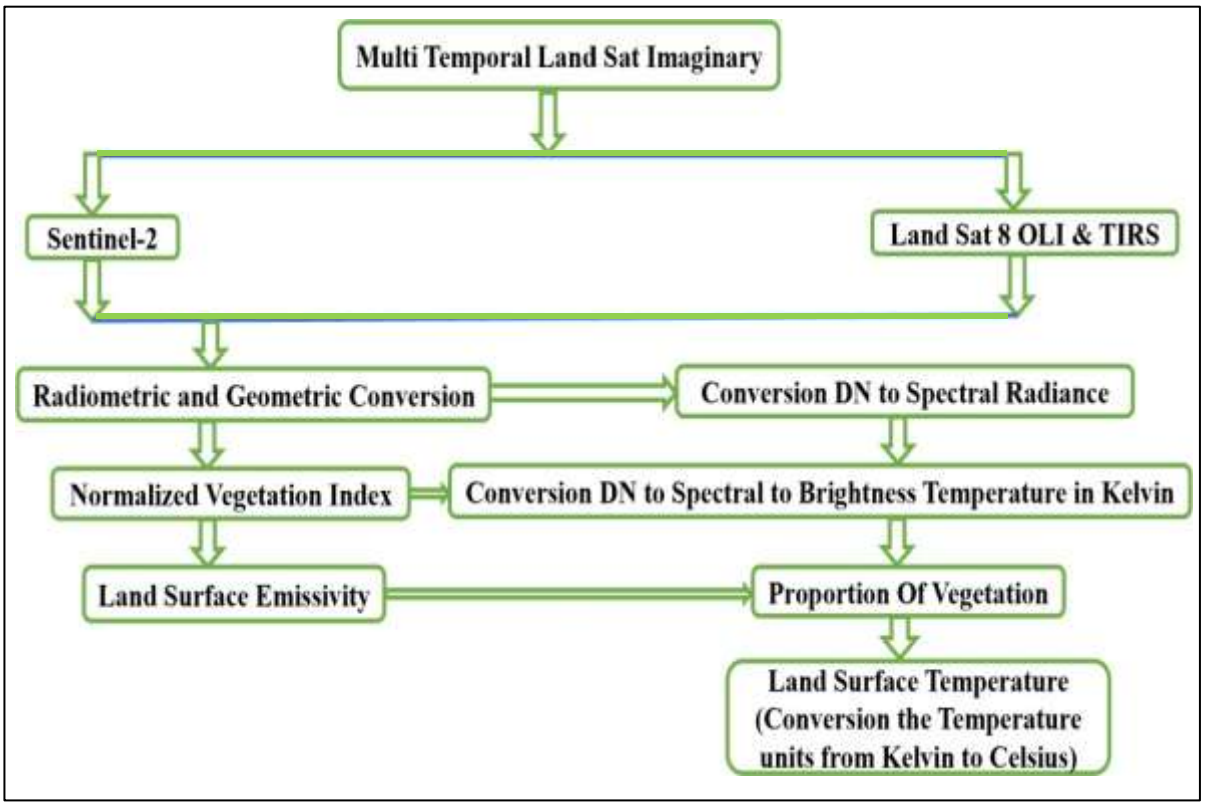


**Fig. 2. General methodology for LST**

**5 Results and Discussions**

LULC Classification at open-cast mine, LULC data were generated for Open Cast Mine for the years 2021 to 2026 with classes including water bodies, trees/forest land, bare land, barren land and mining area (Fig's 3 to 7). For a precise evaluation, opencast mining sites on the categorized data were confirmed using field data.

**Table II. LULC classes change at Open Cast Mine Area (2021 and 2024).**

| Sl.No. | LULC Class Code | Land Cover Class | Area (Ha) (Year 2021) | Area (Ha) (Year 2026) | Increase/Decrease Land usage (Ha) | Overall change (%) |
|---|---|---|---|---|---|---|
| 1 | 01 | Water Bodies | 38.42 | 50.23 | + 11.81 | 23.52 % |
| 2 | 02 | Forest Land/ Vegetation | 49.64 | 28.38 | - 21.26 | 74.91 % |
| 3 | 05 | Build-up Area | 3066.47 | 2489.60 | - 576.87 | 23.17 % |
| 4 | 07 | Bare Ground | 326.51 | 421.54 | + 95.03 | 22.54 % |
| 5 | 11 | Mining Area/ Barren Land | 84.90 | 167.85 | + 82.95 | 49.41 % |

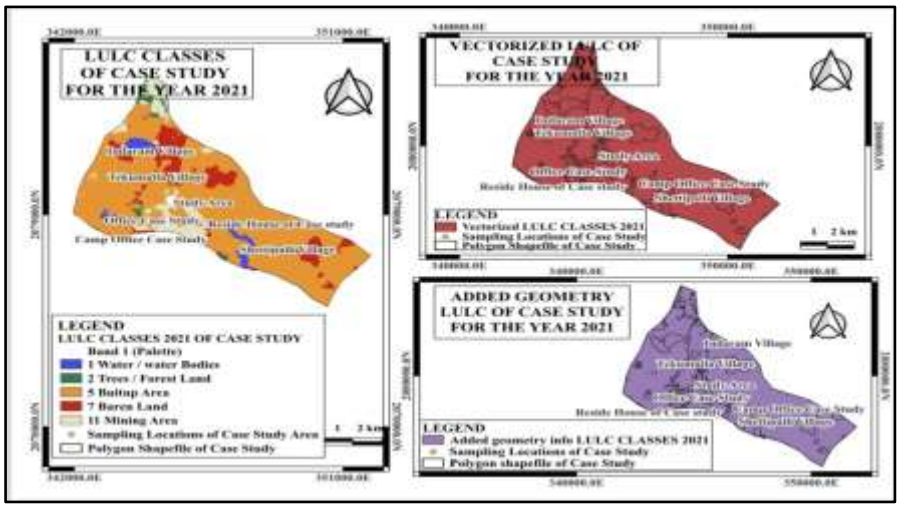



**Fig.3. Sentinel-2 10-Meter Resolution Land Use/Land Cover for the year 2021 for open cast mine area from ESRI (https://livingatlas. arcgis.com/landcover/).**

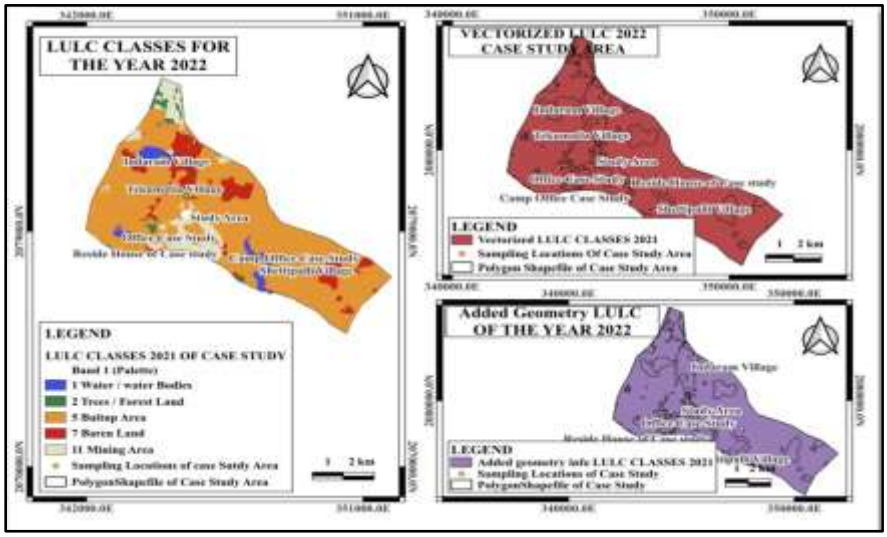


**Fig.4. Sentinel-2 10-Meter Resolution Land Use/Land Cover for the year 2022 for open cast mine area from ESRI (https://livingatlas. arcgis.com/landcover/).**

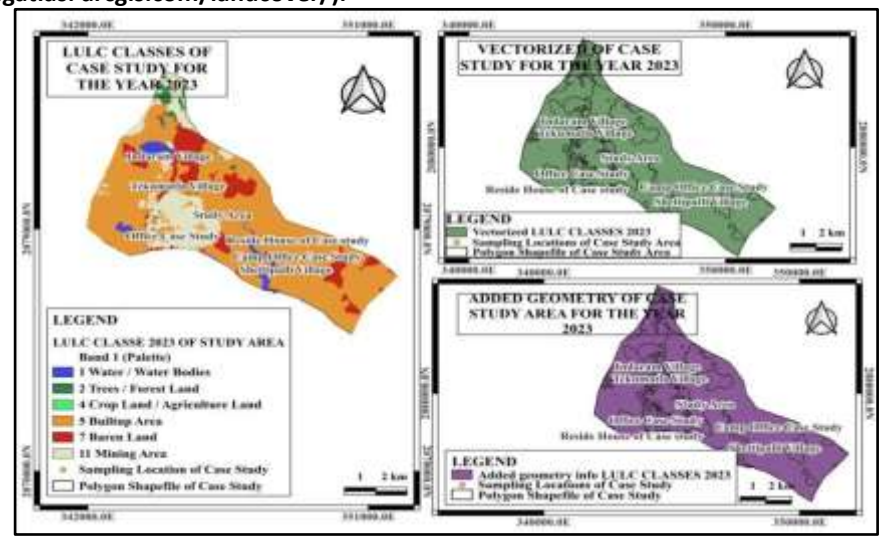



**Fig.5. Sentinel-2 10-Meter Resolution Land Use/Land Cover for the year 2023 for open cast mine area from ESRI (https://livingatlas. arcgis.com/landcover/).**

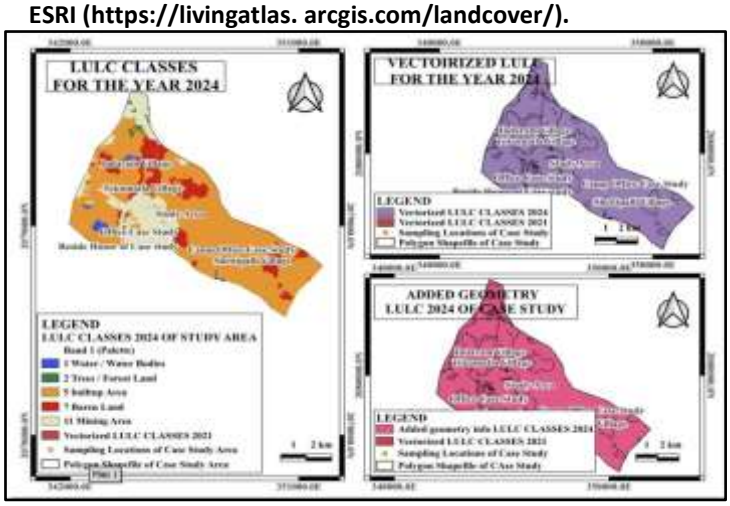



**Fig.6. Sentinel-2 10-Meter Resolution Land Use/Land Cover for the year 2024 for open cast mine area from ESRI (https://livingatlas. arcgis.com/landcover/).**

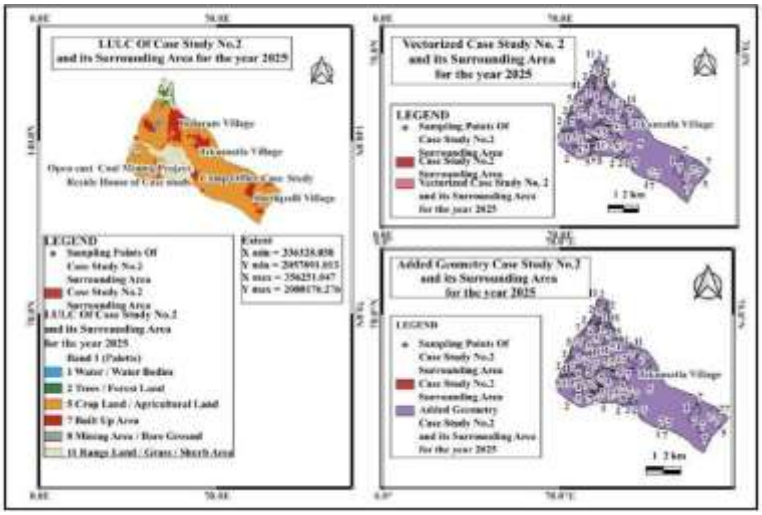


**Fig.7. Sentinel-2 10-Meter Resolution Land Use/Land Cover for the year 2025 for open cast mine area from ESRI (https://livingatlas. arcgis.com/landcover/).**

The LULC analysis showed a sharp increase/decrease in land cover classes in the open cast mining area during 2021 to 2026 (Table II).

- Forest Land/Vegetation (-74.91%) – Crop land is the dominant LULC class, covering 49.64 ha in 2021 to 28.38 ha in 2026. Mining operations may cause conversion and fragmentation of agricultural land through mine expansion, overburden dumping, haul-road construction, and associated infrastructure.
- Built-up Area (-23.17%) – Built-up land occupies 3066.47 ha in 2021 to 2489.60 ha in 2026. Mining-related roads, processing facilities, settlements, workshops, and other infrastructure can contribute to changes and expansion of built-up areas.
- Bare Ground (+22.54%) – Bare ground covers 326.51 ha in 2021 to 421.54 ha in 2026, representing directly disturbed and exposed surfaces with little or no vegetation. Open-cast excavation covering active excavation surfaces and mine benches, overburden dumps, tailings, haul roads and cleared mine surfaces can increase the extent of barren ground.
- Water Bodies (+23.52%) – Water bodies cover 38.42 ha in 2021 to 50.23 ha in 2026. Deep expanded mining operations may influence water resources through drainage alteration, increased runoff, sedimentation, groundwater disturbance, and changes in surface topography.
- Mining Area/Barren Land (+49.41%) – Mining/bare ground covers 84.90 ha in 2021 to 167.85 ha in 2026, representing directly disturbed and exposed surfaces. Open-cast excavation covering overburden removal, waste dumping, stockpiling, and mine expansion can increase the extent of barren and disturbed land.

**Land Surface Temperature (LST) Analysis at Open-Cast Mine Area:**

LST analysis at open cast mine area during 2021 to 2026 (Fig's. 8-13), shows an increasing trend for the time interval from 28–32°C in 2020 to a peak of 38°C in 2022, with the highest values concentrated over the open cast mine area by 2025, the maximum LST further rose to 45°C.

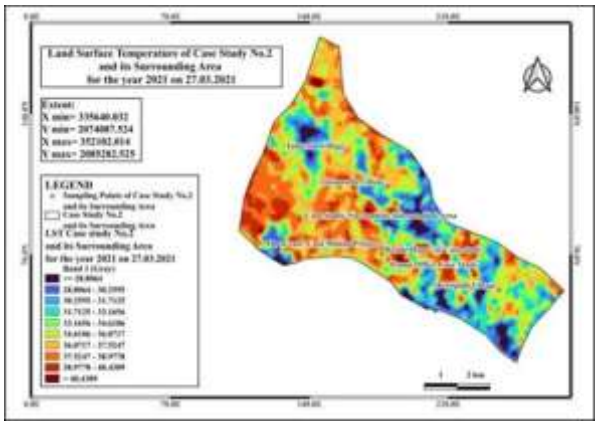



**Fig. 8. LST of open cast mine area for the year 2021 (https://earthexplorer.usgs.gov/).**

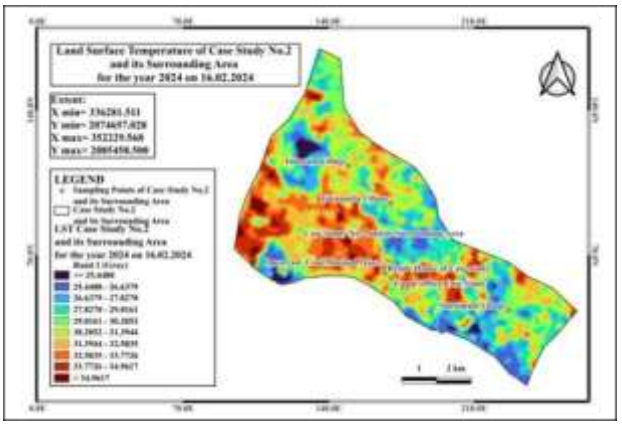
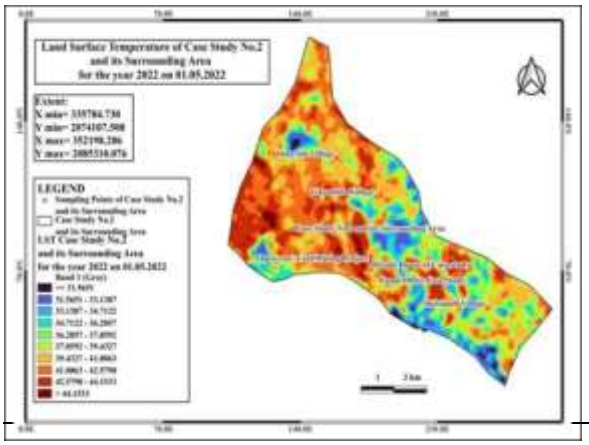



**Fig. 9. LST of open cast mine area for the year 2022 (https://earthexplorer.usgs.gov/).**



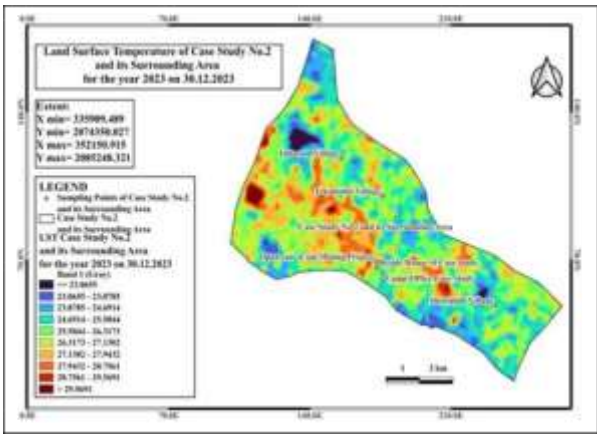



**Fig. 10. LST of open cast mine area for the year 2023 (https://earthexplorer.usgs.gov/).**

**Fig. 11. LST of open cast mine area for the year 2024 (https://earthexplorer.usgs.gov/).**

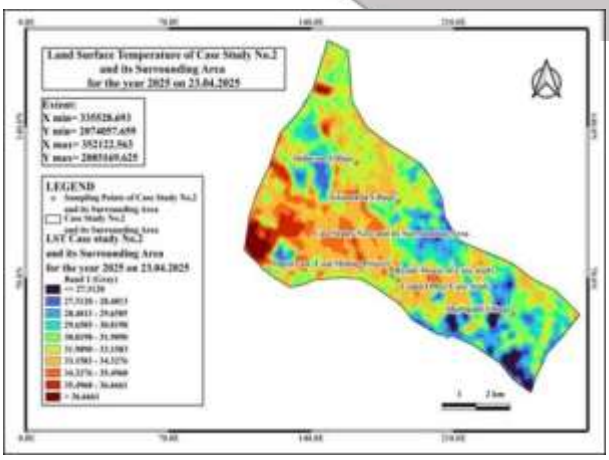



**Fig. 12. LST of open cast mine area for the year 2025 (https://earthexplorer.usgs.gov/).**

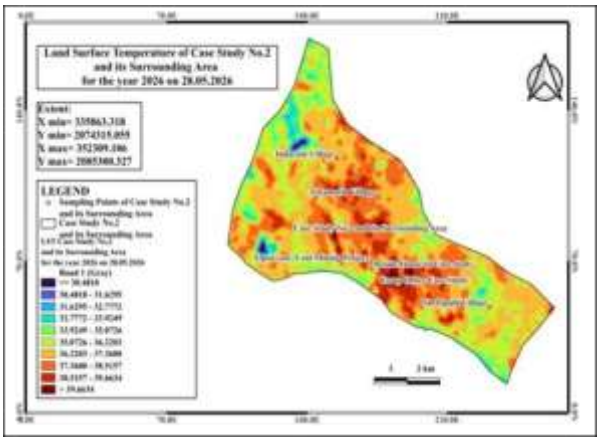



**Fig. 13.. LST of open cast mine area for the year 2026 (https://earthexplorer.usgs.gov/).**

The categorise of five classes: mine pit, overburden dump, vegetation, water bodies and built-up areas recorded an LST values of 40.2°C, 38.7°C, 30.8°C, 27.9°C, & 36.1°C respectively. The LST of nearby buffer zone areas within 5 km was in the range of 35.5°C - 40.2°C. The spatial pattern of hotspot areas remained almost static even as absolute values increased. The upward trend continued in 2025, with high-temperature pixels also appearing in non-mining zones due to industrial and settlement activities. Overall, the temporal rise in LST aligns closely with rapid land use/land cover changes.

**Field LST and Image LST Comparison at Open Cast Mine Area**:

An infrared LCD monitor thermometer was used to measure field LST for validating the remotely derived LST values. Field Land Surface Temperature (LST) in categorise five classes: mine pit, overburden dump, vegetation, water bodies and built-up areas recorded an LST value of 39.5°C, 37.8°C, 31.2°C, 28.4°C & 35.6°C respectively

(Table III). The LST of nearby areas within 5km was identified within the range of 32.5°C - 38.5° with an accuracy of more than 98% (Table IV) (Fig. 14). A strong positive correlation ($R^2$ = 0.9578) exists between mine area expansion and mean annual LST. The fact that NDVI and LST have a negative relationship ($R^2$ = 0.89) indicates that one of the main causes of rising surface temperatures is vegetation removal.




a) Site office b) Indaram Village

c) Nizambad Palle Village d) Shetpalli Village

e) Tekumatla village f) Water Bodies

**Fig. 14. Field LST measurement in different areas**

**Table III. Temperature data by land cover type: Field vs. Image LST at open cast mine area**

| Land Cover | Field LST (°C) | Image LST (°C) | % of Accuracy |
|---|---|---|---|
| Mine Pit | 39.5 | 40.2 | 98.6 % |
| OB Dump | 37.8 | 38.6 | 97.9 % |
| Vegetation | 31.2 | 30.8 | 98.7 % |
| Water body | 28.4 | 27.9 | 98.2 % |
| Built-up | 35.6 | 36.1 | 98.6 % |

**Table IV. LST data by sampling location: Field vs. Image LST at open cast mining area.**

| Sl. No. | Sampling Location | Field LST (°C) | Image LST (°C) | Accuracy (%) |
|---|---|---|---|---|
| 1 | Site office. | 38.5 | 40.2 | 98.2 % |
| 2 | Residential Houses | 37.8 | 38.6 | 97.9 % |
| 3 | Camp Office. | 37.2 | 36.8 | 98.7 % |
| 4 | Indaram Village Houses | 32.5 | 35.5 | 95.5 % |
| 5 | Nizambad palle Village Houses. | 35.6 | 36.1 | 98.6 % |
| 6 | Residential Houses, Shettipalli village. | 35.6 | 36.5 | 98.8 % |
| 7 | Residential Houses, Tekumatla village. | 35.0 | 36.0 | 97.2 % |

# 6 Conclusions

This study shows that the growing area under open-cast coal mining (2021–2026) has a substantial effect on both LULC & LST in the adjoining areas of the Mancherial region, Telangana. Key findings of the study are Water bodies, bare ground, and mining area increased by 11.81 Ha (+23.52%), 95.03 Ha (+22.54%) and 82.95 Ha (+49.41%), respectively, while forest land/vegetation, and build-up area declined by 21.26 Ha (-74.91%) and
576.87 Ha (-23.17%), respectively during the years 2021–2026 for a period of five years. The forest land/vegetation, and build-up area decline due to substantial increase of mining activities during the development period in the mining area, and later increased due to reclamation, backfilling and revegetation activitites at previously disturbed surfaces.

Land Surface Temperature (LST) in the open cast mine area increased from 28°C to 32°C in 2021 to a maximum of 45°C in 2026 for a period of five years. Mine pit, overburden dump, built-up area, vegetation, and waterbodies recorded the field LST of 39.5°C, 37.8°C, 35.6°C, 31.2°C, & 28.4°C, respectively. The LST of nearby areas within 5km was identified within the range of 32.5°C - 38.5°C with an accuracy of more than 98%. A strong positive correlation ($R^2$ = 0.9578) exists between mine area expansion and mean annual LST. A negative correlation between NDVI and LST ($R^2$ = 0.89) confirms that vegetation loss is a key driver of rising surface temperatures.

Appropriate environmental protection measures should be implemented after mining operations. One important way to safeguard the environment and lower the temperature of the air is through reclamation planning. After exploitation is completed, abandoned mine areas should be filled or restored with sand, soil, or water, and afforestation programs should be planned to restore soil fertility. We should actively encourage effective techniques and advanced mining technology to reduce temperature around open-cast coal mining regions, along with education and public awareness.

The results of the study expose the important of spatial and temporal variations in LULC, and LST patterns in the study area. Remote sensing analysis using satellite datasets proved effective in capturing environmental changes associated with mining activities. The findings further suggest that topographic conditions and opencast mining operations play a major role in influencing pollution and subsequent LULC changing aspects. These findings show the potential of geospatial techniques for environmental monitoring and impact continuous assessment in coal mining regions. Spectral band selection, feature optimization techniques, and imaging resolution all have an impact on the study's LULC classification outcomes. The use of a small number of spectral bands and persistent striping in Landsat-8 data may have decreased categorization accuracy, particularly for fine-scale objects. In addition, the lack of socio-economic data limits a fuller understanding of the causes of land use land cover modification brought on by mining, including vegetation, water, and temperature changes in the Mancherial region of Telangana state. Incorporating demographic information can further clarify the industrial and human factors influencing shifts in LULC, thereby enhancing the study's significance to sustainable land usage. In addition, the use of Google Earth Engine's multispectral analysis capabilities can improve pre-processing, support testing of alternative classifiers, and enable the use of images with greater resolution such as Sentinel-2 and Landsat-8. These approaches can strengthen environmental surveillance in open-cast coal mining areas and support informed decision-making and long-term ecosystem conservation and sustainable mining practices in the mining areas.

**Acknowledgement**

Our sincere gratitude to National Institute of Technology Karnataka (NITK), for offering the resources and

assistance needed to carry out the research project in the institute, and thanks to SCCL for conducting studies at the project site.

## References


1. Bisht, D.S, Sridhar, V., Mishra, A., Chatterjee, C., & Raghuwanshi, N.S. (2019). Drought characterization over India under projected climate scenario. International Journal of Climatology, 39(4), 1889–1911. https://doi.org/10.1002/joc.5922
2. Chowdhuri, I., Pal, S.C., Saha, A., Chakrabortty, R., & Roy, P. (2021). Evaluation of different DEMs for gully erosion susceptibility mapping using in-situ field measurement and validation. The Journal Ecological Informatics, 65,101425. https://doi.org/10.1016/j.ecoinf.2021.101425
3. Gond, A.K,, Jamal, A., & Verma, T. (2026). Investigation of land use and land cover using Google Earth Engine machine learning algorithms surrounding a major open cast coal mining complex, Chhattisgarh, India. Journal of the Indian Society of Remote Sensing, 54,1225–1242. https://doi.org/10.1007/s12524-025-02317-6
4. Gorai, A.K. (2022). Sensitivity analysis of GIS-based fuzzy-AHP model for prediction of slope failure susceptibility index. Journal of the Indian Society of Remote Sensing, 50, 715–733. https://doi.org/10.1007/s12524-021-01471-4
5. Ji, H., & Luo, X. (2021). Implementation of ensemble deep learning coupled with remote sensing for the quantitative analysis of changes in arable land use in a mining area. Journal of the Indian Society of Remote Sensing, 49, 2875–2890. https://doi.org/10.1007/s12524-021-01403-2
6. Kumar Reddy, S (2023). Analysis of faults' effect on the highwall stability of Medapalli Open Pit Coal Mine. Geotechnical and Geological Engineering, 41, 2969–2986.
7. Kumar Reddy, S.,,Sastry, V.R. (2016). Stress Distribution on Blasting Gallery Barrier Pillar due to Goaf Formation During Extraction, Journal of The Institution of Engineers (India): Series D, 97(2), 205–213.
8. Liu, B., Pan, L., Qi, Y., Guan, X., & Li, J. (2021). Land use and land cover change in the Yellow River Basin from 1980 to 2015 and its impact on ecosystem services. Land 10(10), 1080. https://doi.org/10.3390/land10101080
9. Lokesha, E.B., Mangalpady, A., Kumar Reddy, S., & Srinivasa, A. S. (2023). Development of Regression Model and Optimization of Mechanical Properties of Geopolymer Concrete Prepared Using Gold Ore Tailings, Journal of Hazardous, Toxic, and Radioactive Waste , 27(4), 04023033.
10. Lokesha, E.B., Mangalpady, A., & Kumar Reddy, S. (2025). Durability characteristics of geopolymer concrete produced using gold ore tailings along with recycled coarse aggregates, Scientific Reports, 15(1), 12051.
11. McConnell, W.J., & Moran, E.F. (2002). Meeting in the middle: the challenge of meso-level integration. Land Use Policy, 19(2), 99–101. https://doi.org/10.1016/S0264-8377(02)00012-1
12. Mishra, R.K., Pandey, J.K., & Pandey, J. (2020). Detection and analysis of coal fire in Jharia Coalfield (JCF) using Landsat remote sensing data. Journal of the Indian Society of Remote Sensing, 48, 181–195. https://doi.org/10.1007/s12524-019-01059-4
13. Nugroho, G., Sofan, P., & Pambudi, A.I. (2023). Improving open-pit mining mapping accuracy in the tropics using enhanced input selection for classification process of machine learning. Journal of the Indian Society of Remote Sensing, 51, 2481–2494. https://doi.org/10.1007/s12524-023-01771-7
14. Reddy, S.K. (2023). Monitoring and prediction of slope failure instability in a limestone mine. Mines, Metals & Fuels, 71(2), 163–170.
15. Shelestov, A., Lavreniuk, M., Kussul, N., Novikov, A., & Skakun, S. (2017). Exploring Google Earth Engine platform for big data processing: classification of multi-temporal satellite imagery for crop mapping. Frontiers in Earth Science, 5, 1-10. https://doi.org/10.3389/feart.2017.00017
16. Tamiminia, H., Salehi, B., Mahdianpari, M., Quackenbush, L., Adeli, S., & Brisco, B. (2020). Google Earth Engine for geo-big data applications: a meta-analysis and systematic review. ISPRS Journal of Photogrammetry and Remote Sensing, 164, 152–170. https://doi.org/10.1016/j.isprsjprs.2020.04.001
17. U.S. Geological Survey (USGS) (2026) EarthExplorer. Available at: https://earthexplorer.usgs.gov/. Accessed 16 Jun 2026.
18. Venter, Z.S., Barton, D.N., Chakraborty, T., Simensen, T., & Singh, G. (2022). Global 10 m land use land cover datasets: a comparison of Dynamic World, World Cover and Esri Land Cover. Remote Sensing, 14, 4101. https://doi.org/10.3390/rs14164101
19. Wang, C., Wang, Y., Wang, R., & Zheng, P. (2018). Modelling and evaluating land-use/land-cover change

for urban planning and sustainability: a case study of Dongying City, China. Journal of Cleaner Production, 172, 1529–1534. https://doi.org/10.1016/j.jclepro.2017.10.294

20. Workie, T.G., & Debella, H.J. (2018). Climate change and its effects on vegetation phenology across ecoregions of Ethiopia. Global Ecology and Conservation, 13, e00366. https://doi.org/10.1016/j.gecco.2017.e00366